

SHEAR BEHAVIOR OF REDUCED MODULUS PRESTRESSED HIGH-STRENGTH SELF-CONSOLIDATING CONCRETE (HS-SCC) MEMBERS SUBJECTED TO ELEVATED CONCRETE FIBER STRESSES

Jared E. Brewer, PhD, CTL Group, Skokie, IL

John J. Myers, PhD, PE, Missouri University of Science and Technology, Rolla, MO

ABSTRACT

Increasing the stress limits at release of prestressing has garnered significant interest recently. Stress limits are used to provide adequate serviceability performance and to prevent premature failure of the materials. As engineers continue to push the envelope on span length and girder spacing to reduce costs, bridge girders are subjected to increasingly higher levels of stress under service loading. The impact of increasing the stress limits at release of prestressing would be to increase the amount of steel a given section can contain, to reduce or eliminate the need for draping or debonding of strands improving plant safety and to provide faster turn around for precast plants since prestressing could be released at lower concrete strengths. In addition to increasing the stress limits, an increasing number of precast plants would like to be able to reap the benefits of self-consolidating concrete, but are reluctant due to the relatively unknown behavior of the material in prestressing applications.

For this program, six reduced scale prestressed concrete girders were cast with targeted release stresses between 60% and 80% of the initial concrete compressive strength. Time-dependant prestress losses were measured at regular intervals for 196 days, which was then followed by structural testing to failure. Three of the girders were designed and tested for flexural performance, while the other three were designed and tested for shear performance. This paper reports the results of six shear tests conducted in the Structural Engineering Research Laboratory at Missouri S&T on the high-strength self-consolidating concrete members.

Keywords: Stress limits, elevated fiber stresses, high-strength self-consolidating concrete, reduced modulus concrete, shear behavior, shear strength.

INTRODUCTION

The necessity of stress limits for prestressed concrete members has recently been subjected to scrutiny. These limits have typically been employed as a check on serviceability performance and material failure. With the development of advanced materials the limitations may no longer be applicable or appropriate. Increasing the stress limits at prestress release can result in sections containing an increased percentage of steel and can reduce or eliminate the need for draping or debonding of strands. Self-consolidating concrete (SCC) can also provide additional benefits for the precast/prestress industry but the limited experience has hampered the use in many structural members. Therefore, this investigation studied the prestress loss behavior and structural performance of prestressed concrete girders produced with high-strength self-consolidating concrete (HS-SCC) subjected to elevated compressive fiber stresses at release of prestressing.

HIGH-STRENGTH SELF-CONSOLIDATING CONCRETE (HS-SCC)

High-Strength Concrete (HSC) is now widely accepted by the prestressed/precast concrete industry. It has many advantages, including reduced material requirements resulting from the use of more compact sections. It also permits longer girder spans and increased girder spacing, thereby reducing material and total bridge costs. SCC is gaining wider acceptance due its performance characteristics in the fresh state. It can eliminate the need for vibration, which reduces fabrication time and labor costs, and it has a reduced potential for segregation, voids, and surface defects. Due to these advantages, a combination of SCC performance characteristics and HSC material properties would result in an attractive material for the construction industry.

Although the fresh properties of SCC are beneficial, the effect on hardened properties can be detrimental. Research has indicated that SCC has reduced modulus of elasticity (MOE) values compared to conventional normal-strength or high-strength concretes^{1,2}. This reduced MOE can be attributed to the lower coarse aggregate contents often specified to obtain the required rheological characteristics of SCC¹. It is common for HSC mixes to use significantly more coarse aggregate than SCC mixes, resulting in higher MOE levels³.

Influential in the shear capacity of conventional concrete is the development of aggregate interlock. For normal strength concrete, the size and volume of coarse aggregate will affect the shear capacity due to the interlocking of aggregates on the crack surface. According to Walraven and Stroband⁴, the general principle is that due to the roughness of the crack surface from the aggregates, a wedging action is developed due to the shear force. They found that for high strength concrete the shear friction is significantly reduced due to fracture of the aggregate particles⁴. Therefore, HS-SCC has the effect of reduced coarse aggregate contents as well as higher compressive strengths, which can lead to a reduced influence of aggregate interlock on the shear capacity. Kim et al.⁵ found that SCC with 16-hour release strengths of 5 and 7 ksi (34.5 and 48.3 MPa) exhibited less aggregate interlock than comparable strength conventional concrete. Their current information was inconclusive on the need for additional shear reinforcement in girders produced with SCC.

Full scale testing of SCC girders performed by Naito et al.² was used to evaluate the nominal flexural and shear strengths. The SCC girders performed comparatively to high early-strength concrete (HESC) girders produced with similar materials. They noted that material properties of their SCC outperformed current industry recommendations², but that the conclusions applied only to the specific mix used in that project and further testing of other SCC mixes is needed.

STRESS LIMITS

Currently, *AASHTO LRFD Bridge Design Specifications*⁶ (hereafter called *AASHTO LRFD*) Article 5.9.4.1.1 limits the extreme fiber stress in compression to 60% of the concrete compressive strength ($0.6f_{ci}'$) immediately after prestress transfer. *ACI 318-08 Building Code Requirements for Structural Concrete*⁷ (hereafter called *ACI 318*) Section 18.4.1 limits the extreme fiber stress in compression at midspan to $0.6f_{ci}'$, but it has been updated to permit $0.7f_{ci}'$ at the ends of the member. The *PCI Standard Design Practice*⁸ states that "it has been common practice to allow compression up to $0.70f_{ci}'$ " while referencing work by Noppakunwijai et al.⁹ demonstrating that the limits are conservative. The intent of stress limits are to maintain serviceability, as noted in the *ACI 318* commentary, by preventing excessive deformation and to minimize cracking. Compression stress limits also appear to serve as an indirect means to ensure that crushing of concrete does not occur at prestress transfer⁹. Numerous projects have investigated the necessity for these allowable stress limits, all typically reach a similar conclusion that increasing the compression stress limit to at least $0.7f_{ci}'$ is feasible.

RESEARCH PROGRAM

This program cast six reduced scale prestressed concrete girders with targeted compressive fiber stresses between 60% and 80% of the initial concrete compressive strength at release of prestressing. Time-dependant prestress losses were measured at regular intervals for 196 days. Girders then were subjected to load in structural testing to failure with three of the girders designed and tested for flexural behavior, while the other three were designed and tested for shear behavior. Additional background information and the results of the time-dependant prestress loss study has been previously published¹⁰.

CONCRETE MATERIALS

The precast concrete supplier used a Missouri Department of Transportation (MoDOT) approved HS-SCC mix. This mix is typically used for MoDOT projects requiring higher compressive strength SCC. The design target compressive stresses were 8 ksi (55 MPa) at release of prestressing and 10 ksi (69 MPa) at 28 days. All six girders were cast simultaneously from the same batch; thus material properties were consistent. The mixture proportions used for this project are presented in **Table 1**. For mechanical property testing, 4 in. x 8 in. (100 mm x 200mm) cylinders were cast and stored with the girders until test age.

Table 1 – Mixture Proportions

Mix Constituent Materials		Description
Cement	777 lb/yd ³	ASTM Type III Portland Cement
Coarse Aggregate	889 lb/yd ³	Crushed Limestone – ¾ inch MAS
Intermediate Aggregate	460 lb/yd ³	Crushed Limestone Chips - ⅜ inch MAS
Fine Aggregate	1419 lb/yd ³	ASTM C 33 - Natural River Sand
HRWR	90 oz/yd ³	ASTM C 494 Type F - Polycarboxylate
Air Entrainment	12 oz/yd ³	ASTM C 260 – Neutralized Vinsol Resin
Water-Cementitious Ratio	0.369	–

Note: 1 lb/yd³ = 0.5933 kg/m³, 1 inch = 25.4 mm, 1 oz/yd³ = 38.69 mL/m³

In general, SCC can be produced using standard concrete aggregates, as long as aggregate gradation is considered when developing the SCC mix design. To produce a mix with the rheological characteristics of SCC while avoiding segregation problems, a uniform gradation is typically employed to minimize the voids between the aggregates. For the mix used here, the coarse aggregate was a locally available crushed limestone with a maximum aggregate size of ¾ in. (19 mm). The combination of these particle size distributions produced a gap graded mix with a lack of particles in a sieve range from the No. 4 sieve to ⅜ in. (9.5 mm). To fill the gaps and achieve a uniform gradation, crushed limestone chips with a maximum size of no more than ⅜ in. (9.5 mm) were used. The resulting combination of fine and coarse aggregates produced a well graded distribution resulting in a smaller volume of voids.

The mix proportions indicate that the total coarse aggregate fraction (¾ in. (19mm) plus ⅜ in. (9.5 mm) chips) was 34.9% by weight. Typical high-strength concrete mixes have on average 45% coarse aggregate content³. Schindler et al.¹¹ reported the average coarse aggregate fraction of SCC mixes as 43%, with a low of 38.5%. These indicate that the coarse aggregate content used in the present study was below that normally found in most HSC and SCC mixes and could result in compressive strength and MOE reductions.

GIRDER DESIGNS

The girders were designed using provisions from *AASHTO LRFD*, *ACI 318* and the *PCI Design Handbook, Sixth Edition*. The only provision that was disregarded was the compressive fiber stress limits; all other provisions, including allowable tension limits, were followed. For simplicity of fabrication, all six prestressed girders were cast simultaneously on the same prestressing bed. This simultaneous casting produced an identical prestressing layout and jacking level for every member designed to avoid variations in fabrication. A typical cross-section is shown in **Figure 1**, with sectional properties for the three shear test girders shown in **Table 2**. To achieve higher fiber stresses, the entire section width was reduced in increments, resulting in a reduced area and moment of inertia, which in turn resulted in greater strand eccentricity leading to the higher stresses. As indicated by the test results, the target compressive strength at release of prestressing was not achieved, resulting in higher compressive fiber stresses than anticipated. Thus the label used for each beam in the results and discussion below corresponds to the actual percentage of concrete fiber stress. Each girder was cast to a length of 15 ft (4.57 m) to ensure full development of prestressing.

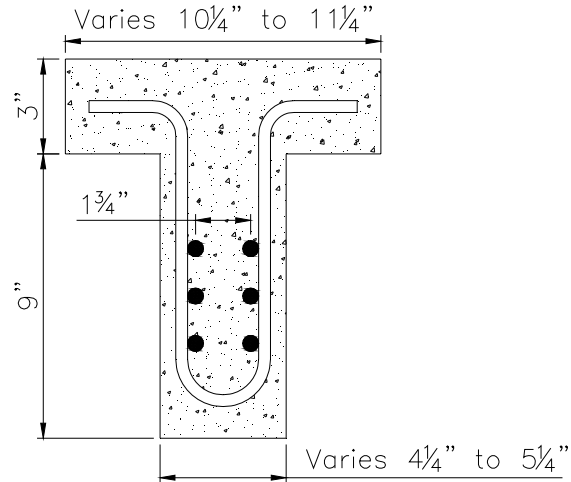


Fig. 1 – Typical Cross-Section

Table 2 - Beam Cross-Sectional Properties

Girder Designation	B-79	B-71	B-65
Target Stress Level (% of f_{ci})	75	68	60
Actual Stress Level (% of f_{ci})	79	71	65
Gross Area, A_g (in²)	69	75	81
Gross Moment of Inertia, I_g (in⁴)	895	975	1053
Distance from CGC to Top Fiber, y_t (in)	4.83	4.92	5.00
Distance from CGC to Bottom Fiber, y_b (in)	7.17	7.08	7.00
Strand Eccentricity, e_p (in)	2.67	2.58	2.50
Distance from Top Fiber to CGS, d_p (in)	7.50		

Note: CGC = center of gravity of concrete, CGS = center of gravity of steel; 1 in. = 25.4 mm

The flexural reinforcement was designed using strain compatibility with a linear-elastic analysis. The resulting longitudinal reinforcement consisted of six ½ in. (12.7 mm) diameter, low-relaxation prestressing strands. All strands were straight and fully bonded to the concrete, and all had a manufacturer reported MOE of 28,500 ksi (197,000 MPa). The strands were jacked to 75% of the ultimate strength by the precaster, resulting in an initial stress before any loss of 202.5 ksi (1396 MPa). Elongation measurements taken before and after jacking were used to determine the initial jacking stress.

The detailed method of analysis found in *ACI 318* was used for the shear design due to the improved accuracy of the results. The detailed approach accounts for two types of inclined cracking that can result in a shear failure: flexural-shear and web-shear cracking. Flexural-shear cracking occurs after flexural cracking has taken place, and can lead to shear-compression failure if not properly reinforced. A shear-compression failure occurs when the compression area at the top of the beam, reduced by diagonal tension cracks, is not sufficient to resist the forces resulting from flexure. Web-shear cracking initiates in the web without flexural cracking and can occur in thin webs of highly prestressed beams. For simply supported beams, web-shear cracking typically starts below the neutral axis. This type of

inclined cracking is less common than flexural shear cracking. Web-shear cracking occurs when the diagonal (principal) tension stresses reach the tensile strength of the concrete at the center of gravity of the section. Calculations showed that the shear force required to cause flexural-shear cracking was lower than that required to cause web-shear cracking and must, therefore, control the design of shear reinforcement.

Transverse shear reinforcement was designed to accommodate the deficiency in shear capacity, with open-ended U-stirrups (see **Figure 1**) produced from mild steel. One end of each girder designed for shear testing contained no shear reinforcement, whereas the other end contained stirrups with different spacing, as shown in **Figure 2**. Since this set of girders would be tested in a reduced span, additional closely spaced reinforcement was included at midspan to ensure failure of the ends. The end with no shear reinforcement was designed to test the contribution of concrete and prestressing to the shear performance; the other end tested the additional contribution of shear reinforcement.

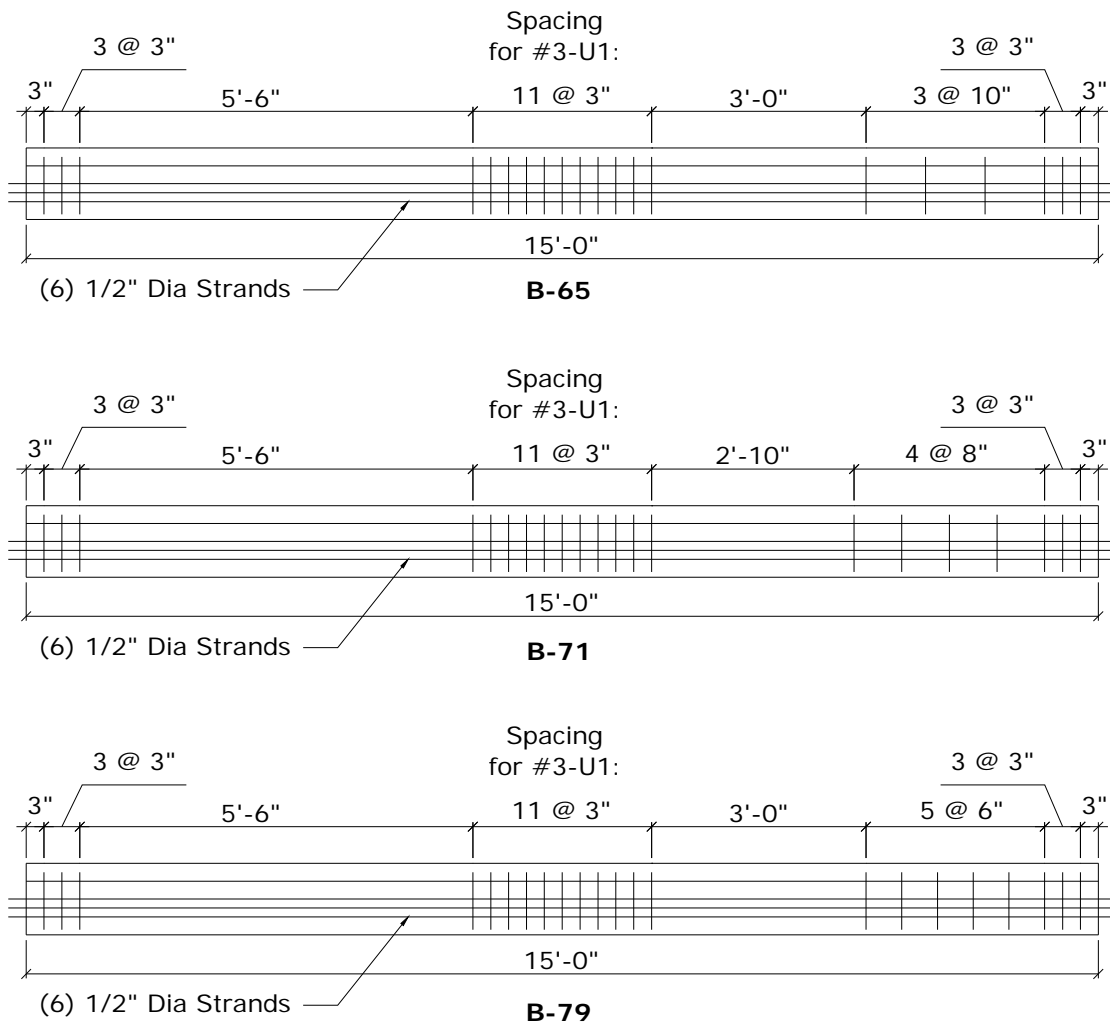


Fig. 2 – Shear Stirrup Spacing for Shear Girder Tests

When high levels of prestress are applied to members, bursting cracks can develop at the ends due to tensile stresses developed within the prestress anchorage zone. These tensile stresses develop perpendicular to the prestressing compressive forces, and when they exceed the tensile strength of concrete, cracks develop. *AASHTO LRFD* Article 5.10.10.1 addresses anchorage zones in pretensioned concrete members. It requires enough vertical reinforcement in the end zone to provide resistance of at least 4% of the total prestressing force at transfer. The factored bursting resistance of the anchorage zone is calculated from the following equation:

$$P_r = f_s A_s \quad (1)$$

where f_s = the steel stress and is not to exceed a maximum working stress of 20 ksi (137 MPa); and A_s = the area of steel to be placed within a distance of $h/4$ from the end of the member. To resist these bursting stresses, an additional stirrup was placed at both ends of each girder, as illustrated in **Figure 2**.

SHEAR TEST SETUP

For each of the three girders tested in shear, two separate tests were performed. The first test was performed to determine the concrete and prestressing contribution to the performance, and the second test examined the shear reinforcement contribution to the performance. The span length was 9 ft (2.74 m) with the support located 3 in. (75 mm) from the end of the member. The load was applied with a hydraulic jack located at midspan, and separated into two point loads located 12 in. (458 mm) from midspan by a spreader beam. Both shear testing setups are shown in **Figure 3**. For all tests, the load was applied at a rate of 1000 lb/sec (4.45 kN/sec) until failure. The load-deformation relationship was measured using a load cell placed under the hydraulic jack, and linear variable differential transformers (LVDT) located at midspan and at under each of the applied loads.

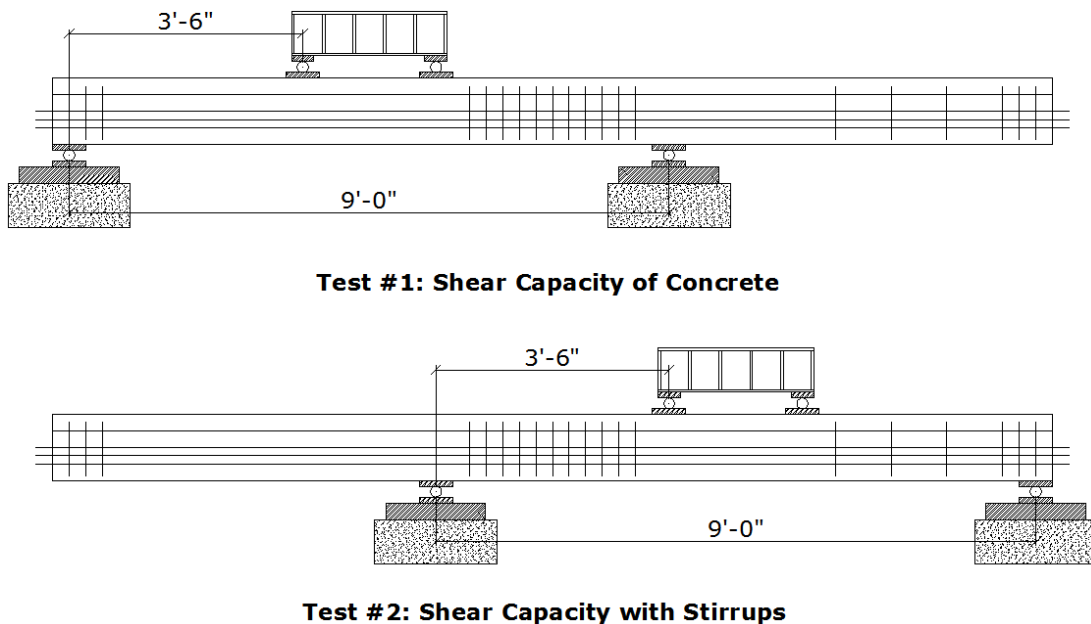


Fig. 3 – Shear Test Setup

EXPERIMENTAL RESULTS

FRESH CONCRETE PROPERTIES

At concrete placement, fresh concrete properties were measured following applicable ASTM standards and the PCI SCC Guidelines¹²; test results are shown in **Table 3**. The SCC slump flow was evaluated using the inverted-slump-cone spread test with a result of 27 in. (68.5 cm). This value was slightly above the targeted range of 22 – 26 in. (56 – 66 cm) but did not result in segregation of the mix. The concrete temperature, air content, and density were typical of normal prestressed SCC members for MoDOT projects.

Table 3 – Fresh Concrete Properties

Fresh Concrete Properties	Test Result
Spread (in)	27
Concrete Temperature (°F)	70
Air Content (%)	6.8
Unit Weight (lb/ft ³)	138

Note: 1 in. = 25.4 mm, °C = (5/9)(°F-32), 1 lb/ft³ = 16.02 kg/m³

HARDENED CONCRETE PROPERTIES

Concrete mechanical properties were tested at release of prestressing (3 days), 28 days, 56 days, and at test age (243 days). Concrete compressive strength at 3 days was found to be 7088 psi (48.8 MPa). The 28-day compressive strength was 9026 psi (62.2 MPa), with an MOE of 4635 ksi (31940 MPa). The concrete strength at 243 days was found to be 8210 psi (56.6 MPa) with an MOE of 4175 ksi (28785 MPa). **Table 4** presents the average, coefficient of variation, and number of concrete cylinder tests at 28, 56, and 243 days. A reduction in cylinder compressive strength of nearly 10% between 28 days and 243 days can only be explained by the improper calibration of testing machines. The 28 and 56 day tests were performed on a Forney compression machine, and the 243 day tests were split, with three tests on the Forney machine and three on a Tinius-Olsen testing machine. Between the 56 and 243 day tests, the Forney machine was recalibrated, which likely caused the change in strength measurements. Since the target strength was not reached, the values of the compressive fiber stresses exceeded values specified in the design as shown in **Table 2**.

Table 4 – Hardened Concrete Properties

Test Age	28 days	56 days	243 days
Average Compressive Strength (psi)	9026	9024	8210
Coefficient of Variation	0.80%	1.41%	1.94%
Number of Compression Tests	3	3	6
Average MOE (ksi)	4635	–	4175
Predicted MOE ¹ (ksi)	5082	–	4847
Ratio of Measured to Predicted MOE	0.912	–	0.861

Note: 1 ksi = 6.89 MPa, 1 – According to AASHTO LRFD 5.4.2.4

The MOE at both 28 and 243 days was significantly lower than anticipated, which affected the prestress loss behavior of the members. The MOE predicted according to *AASHTO LRFD* Article 5.4.2.4 is presented in **Table 4**, along with the ratio of measured to predicted values. As discussed above, a reduced value was expected due to the low coarse aggregate fraction, but this value was even lower than anticipated.

PRESTRESS LOSS BEHAVIOR

The development of prestress losses over time was measured and has been previously reported¹⁰. Since the effective prestressing force is tied directly to the amount of prestress loss, accurate determination of those losses will affect the accuracy of the design predictions. In each of the following shear analyses, the effective prestressing force was determined by two means: first using the predicted prestress losses determined from the Refined Estimates Method of *AASHTO LRFD*, then with the prestressed losses measured in Phase 1 of this research program¹⁰. The *AASHTO LRFD* Refined Estimates Method was selected because it is commonly used throughout the industry. For the purposes of this discussion, the total prestress loss measured at test age and the predicted losses are shown in **Table 5**.

Table 5 – Measured versus Predicted Prestress Losses

Total Losses at 243 days (ksi)			
Designation	B-79	B-71	B-65
Measured	70.7	62.9	57.7
<i>AASHTO LRFD</i>	56.3	52.2	48.6

Note: 1 ksi = 6.89 MPa

PREDICTED SHEAR BEHAVIOR

Both *AASHTO LRFD* and *ACI 318-05* use empirical equations to determine the contribution of concrete, whether prestressed or non-prestressed, to the total shear capacity of the member. Since the shear capacity of concrete is closely related to the mix proportions, and especially to the coarse aggregate content, empirical equations developed for normal strength concrete may not apply to high-strength or self-consolidating concrete. This project determined the shear capacity using the detailed method outlined in *ACI 318* and discussed in the *PCI Design Handbook*. For the girder ends without shear reinforcement, the expected capacity was calculated from the limiting value of web-shear and flexure-shear cracking. For all three girders, flexure-shear was found to be deficient in an area approximately 12 in. (30.5 cm) wide next to the applied concentrated load. For the girder ends with shear stirrups, the limiting shear capacity was lesser in the same area next to the applied load, but it had a larger value due to the contribution from shear reinforcement. The contribution from the shear reinforcement was determined according to *ACI 318* Section 11.5.7.2 which assumes that cracks are inclined at 45°.

The computer program Response-2000¹³ predicts shear capacity based on the Modified Compression Field Theory and was used to analyze the girders with and without shear

reinforcement. The program calculates the capacity at various sections along the girder length and determines the minimum load causing failure.

SHEAR RESULTS

The typical method used to visualize shear behavior is the plot of shear force (or stress) versus shear strain. The shear force was easily determined from load tests, since it is equal to the applied force. The shear strain, however, was not as easily measured since the location of shear failure (i.e., the point where the shear strain was greatest) occurred at varying points along the girders. For simplicity, the shear behavior was plotted as the relationship between load (shear) and displacement at the point of load.

Bursting cracks developed at the ends of the member, reducing the shear capacity of some members. As noted above, the design of prestressed members must be checked to control high tensile forces that develop perpendicular to the prestressing strands and often lead to cracking. For this set of girders, cracking did not occur instantaneously with the release of prestressing, rather, cracks developed as concrete shrinkage and creep added additional stresses. On seven of the 12 member ends, these cracks occurred at one level of prestressing and extended in from the end between 6 and 18 in. (15 and 46 mm). The cause of these cracks was most likely the increased level of prestressing applied to achieve the high fiber stresses demanded by the research program.

The load displacement relationships, both with and without shear reinforcement, are shown in **Figures 4, 5, and 6** for girders B-79, B-71, and B-68, respectively. In each of these figures, the point where the relationship is no longer linear signifies development of shear cracks within the girders, and the transfer of shear to the transverse reinforcement. This point corresponds to a value slightly larger than the shear capacity of the concrete because some of the shear force is already transferred to the transverse reinforcement. **Figure 7** compares the load-displacement relationship for the ends of the girders without shear reinforcement, and **Figure 8** compares the relationship for the ends of the girders with shear reinforcement. Both of these figures indicate little difference in behavior aside from the differing amounts of shear reinforcement.

Figures 9 through 14 show the crack patterns of each of the failed tests. The bursting cracks are visible and their influence on the failure of the girders is apparent. When the bursting cracks extended well into the beam, the shearing forces widen them, and failure extended from them. In members without shear reinforcement, cracks developed beside the support and extended directly to the applied load, similar to deep beam behavior with a direct compression strut. The cracking was typically initiated in the web, indicating web-shear failure, which does not match the design calculations. Due to the small inclination (less than 16°) of the crack and the reinforcement configuration, a strut-and-tie model produced unreliable results. In members with shear reinforcement, flexure cracks developed first, followed by shear cracking through a stirrup, indicating flexure-shear failure as predicted. The crack inclination on these members was approximately 45° , as assumed in the design equation.

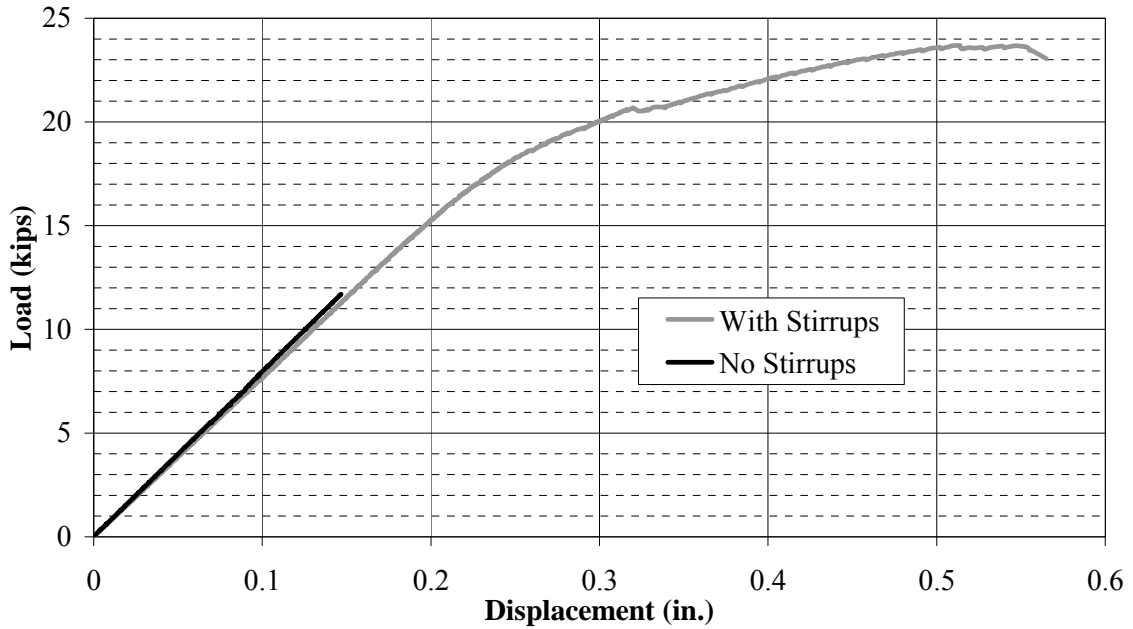


Fig. 4 – Shear Behavior of B-79

Note: 1 kip = 4.45 kN, 1 in. = 25.4 mm

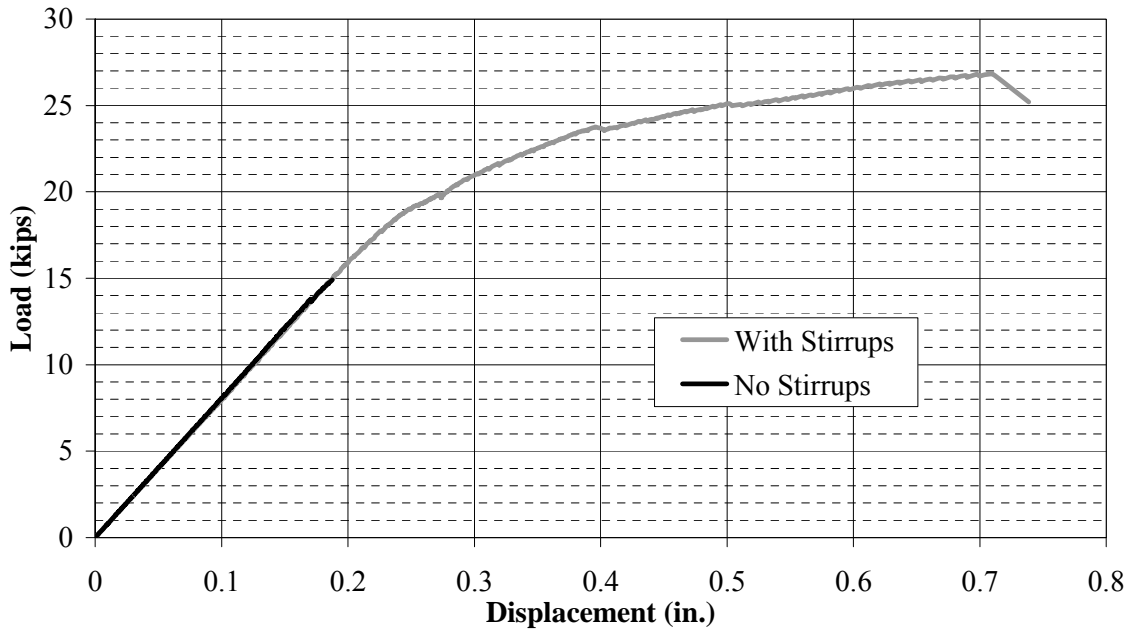


Fig. 5 – Shear Behavior of B-71

Note: 1 kip = 4.45 kN, 1 in. = 25.4 mm

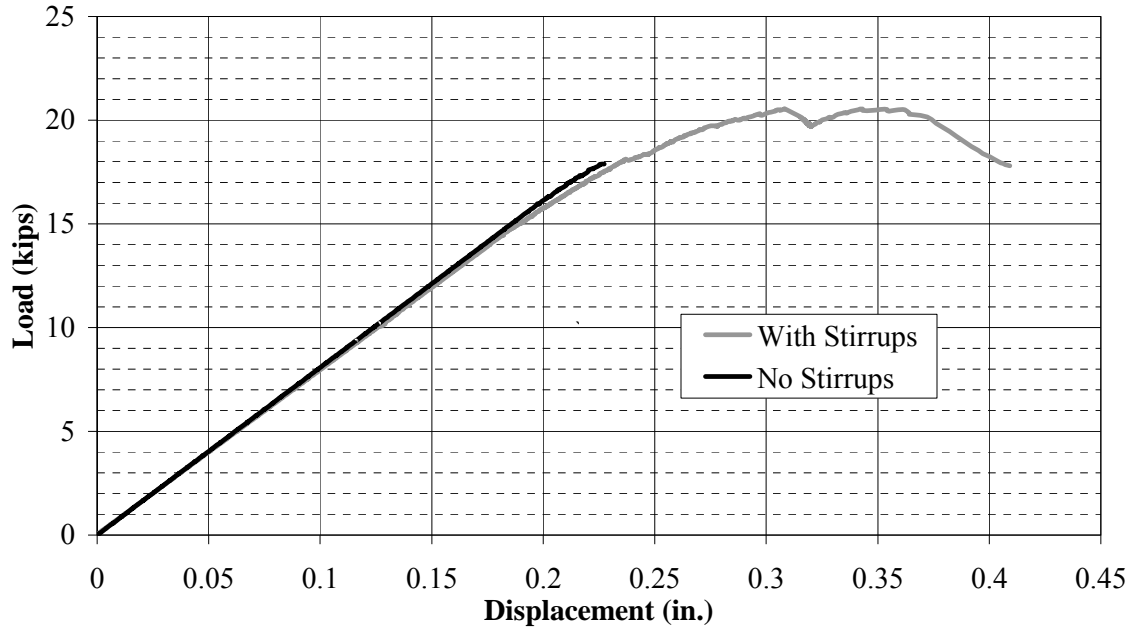


Fig. 6 – Shear Behavior of B-65
 Note: 1 kip = 4.45 kN, 1 in. = 25.4 mm

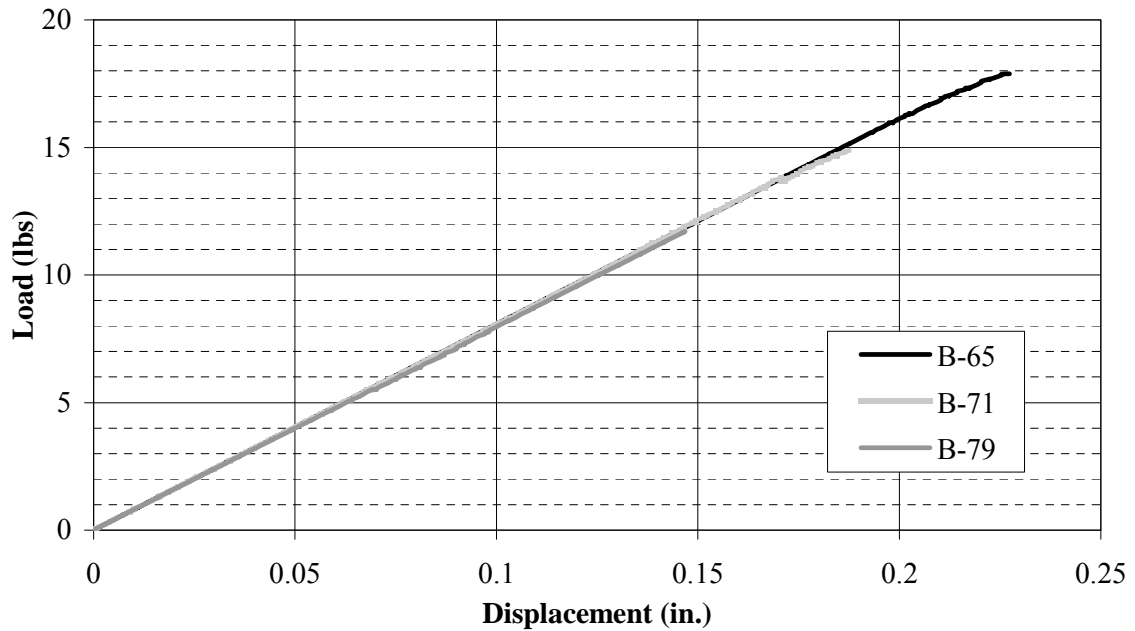


Fig. 7 - Comparison of Shear Behavior without Stirrups
 Note: 1 kip = 4.45 kN, 1 in. = 25.4 mm

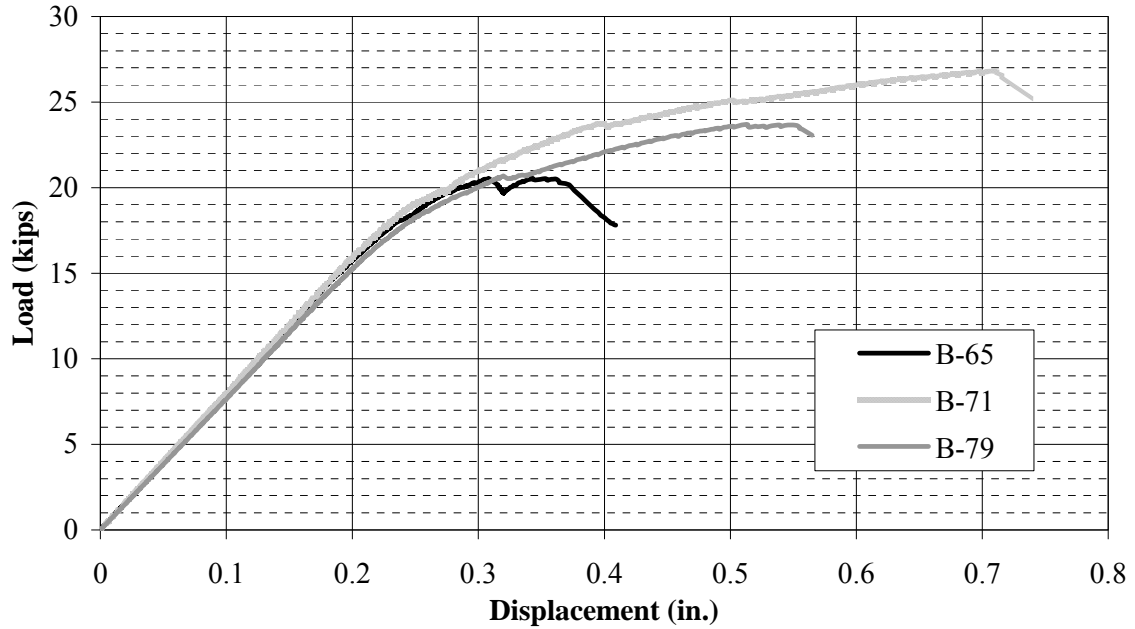


Fig. 8 – Comparison of Shear Behavior with Stirrups

Note: 1 kip = 4.45 kN, 1 in. = 25.4 mm

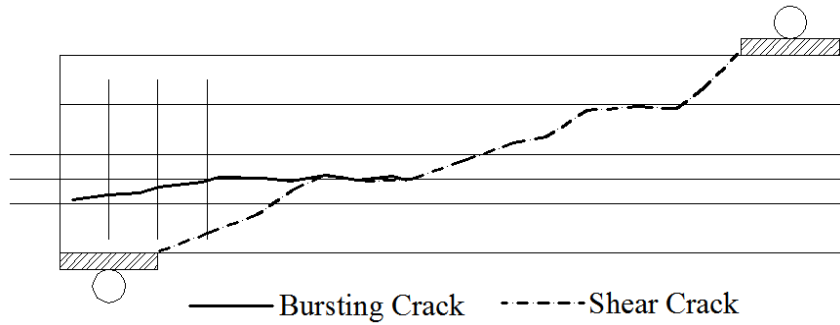


Fig. 9 – Shear Failure of B-65 with No Stirrups

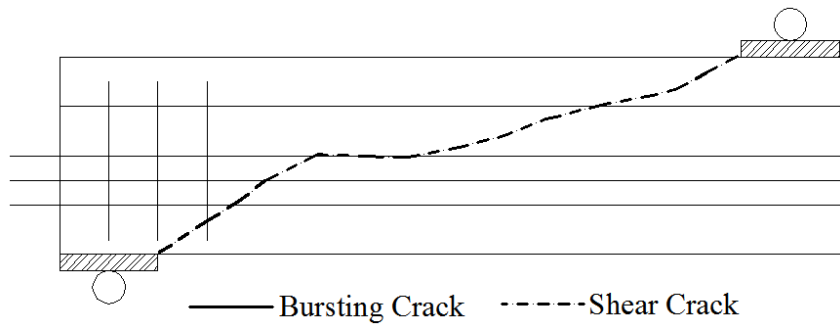


Fig. 10 – Shear Failure of B-71 with No Stirrups

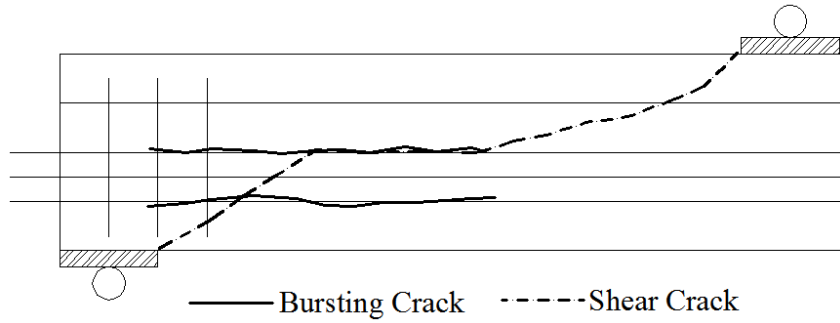


Fig. 11 – Shear Failure of B-79 with No Stirrups

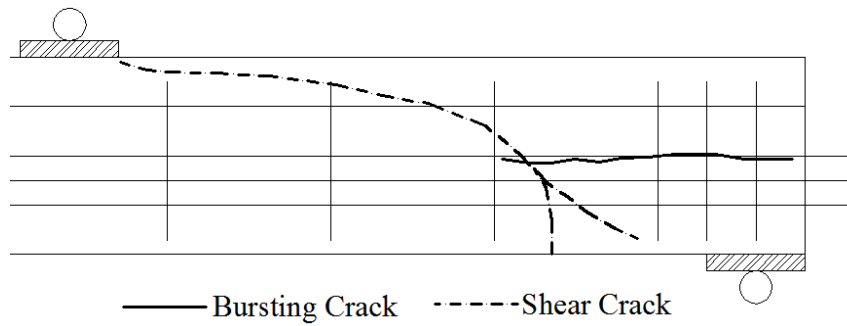


Fig. 12 – Shear Failure of B-65 with Stirrups

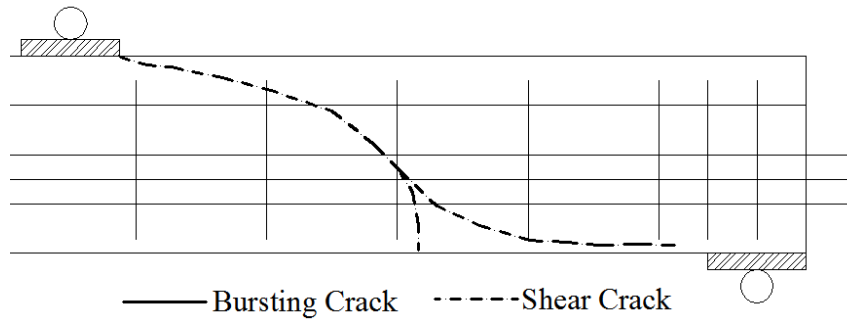


Fig. 13 – Shear Failure of B-71 with Stirrups

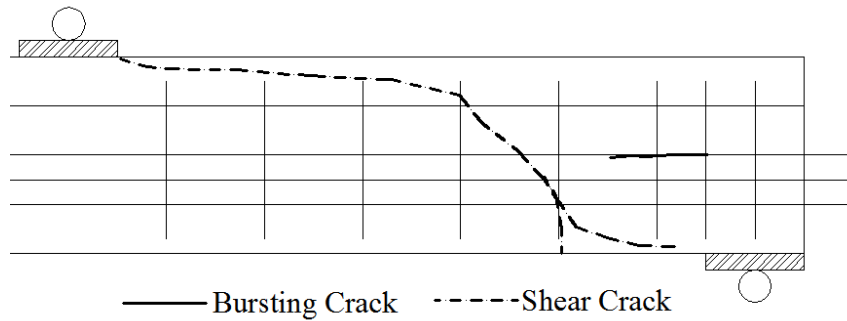


Fig. 14 – Shear Failure of B-79 with Stirrups

Table 6 compares measured shear capacity with the predicted shear capacity outlined above for the ends without shear reinforcement. **Table 7** presents a similar comparison for the ends with reinforcement. Both of these tables indicate that shear failure occurred below the predicted shear capacity in nearly every test. The only underestimation of capacity occurred using the PCI Method on B-65, with an error of 11.6%. For the remaining predictions, the error ranged between 2.4% and 99% overestimation. Test results reported by Naito et al.¹³ showed similar behavior in girders produced with SCC and those produced with HESC, with actual capacity exceeding predicted capacity. The results reported here and the failure patterns shown in **Figures 9** through **14** indicate that, to ensure adequate safety, additional testing is recommended for girders produced using normal and higher strength SCC with lower coarse aggregate contents.

Table 6 – Comparison of Actual versus Predicted Shear Capacity (No Stirrups)

Designation	B-79	B-71	B-65
Shear Failure Load (kips)	11.70	14.91	17.89
Predicted Capacity Using Predicted Losses			
PCI Design Handbook (kips)	15.76	16.18	16.55
Response-2000 (kips)	23.28	24.26	25.20
Predicted Capacity Using Measured Losses			
PCI Design Handbook (kips)	14.48	15.27	15.82
Response-2000 (kips)	21.87	23.35	24.23

Note: 1 kip = 4.45 kN

Table 7 – Comparison of Actual versus Predicted Shear Capacity (Stirrups)

Designation	B-79	B-71	B-65
Shear Failure Load (kips)	23.69	26.82	20.55
Predicted Capacity Using Predicted Losses			
PCI Design Handbook (kips)	32.26	28.55	26.45
Response-2000 (kips)	31.16	29.99	28.28
Predicted Capacity Using Measured Losses			
PCI Design Handbook (kips)	30.98	27.65	24.72
Response-2000 (kips)	30.65	29.72	28.50

Note: 1 kip = 4.45 kN

CONCLUSIONS

Numerous factors affect the structural performance of prestressed concrete members, especially concrete properties. The conclusions drawn here, therefore, are applicable to members produced at the sponsoring production plant in Missouri. The results of the experimental program described here, along with the results from Phase I of this program on prestress losses, suggest the following conclusions:

1. The shear capacity of girders produced using reduced coarse aggregate content HS-SCC is uncertain. Based on the limited results presented here, their capacity is well

- below the capacity predicted using current design equations. Further testing is needed to ascertain the impact of low coarse aggregate content on the shear performance of SCC girders.
2. End region cracking is of concern due to its impact on shear performance. End region cracking should be studied in full-scale SCC girders to evaluate the need for further research, particularly if the use of SCC mixes with reduced aggregate contents is continued to maintain SCC flowability.

ACKNOWLEDGEMENTS

The authors would like to acknowledge the financial support of Coreslab Structures, Inc. in Marshall, Missouri and that of the Center for Transportation Infrastructure and Safety (CTIS) at the Missouri University of Science and Technology (formerly the University of Missouri-Rolla). Thanks are also due to the engineers and personnel at Coreslab Structures, Inc., for their contributions during planning and production. The technician and staff support from the Center for Infrastructure Engineering Studies (CIES) and Department of Civil, Architectural, and Environmental Engineering at the Missouri University of Science and Technology has also provided much appreciated assistance.

REFERENCES

1. Bonen, D.; and Shah, S.; "The Effect of Formulation of the Properties of Self-Consolidating Concrete," *Concrete Science and Engineering: A Tribute to Arnon Bentur*, Proceedings of the International RILEM Symposium, K. Kovler, J. Marchand, S. Mindess, and J. Weiss, eds., RILEM Publications, France, 2004, pp. 43-56
2. Naito, C.J.; Parent, G.; and Brunn, G.; "Performance of Bulb-Tee Girders Made with Self-Consolidating Concrete," *PCI Journal*, V. 51, No. 6, November–December 2006, pp. 72-85
3. Myers, J.J.; "Production and Quality Control of High Performance Concrete in Texas Bridge Structures," Dissertation, University of Texas – Austin, 1998
4. Walraven, J. and Stroband, J.; "Shear Friction in High-Strength Concrete," *Proceedings of ACI International Conference on High Performance Concrete*, Singapore (ACI SP-149), V.M. Malhotra, ed., American Concrete Institute, Farmington Hills, MI (1994), pp. 311-330
5. Kim, Y.H., Trejo, D., and Hueste, M.D.; "Shear Characteristics of Self-Consolidating Concrete for Precast Prestressed Concrete Members," *Self-Consolidating Concrete for Precast Prestressed Applications* (ACI SP-247), A. Schindler, D. Trejo, and R. Barnes, eds., American Concrete Institute, Farmington Hills, MI (2007) pp. 53-65
6. American Association of State Highway and Transportation Officials, *AASHTO-LRFD Bridge Design Specifications*, Fourth Edition, Washington, DC (2007)
7. American Concrete Institute (ACI 318-08), *Building Code Requirements for Structural Concrete*, American Concrete Institute, Farmington Hills, MI (2008)

8. Precast/Prestressed Concrete Institute, *PCI Design Handbook, Precast and Prestressed Concrete*, Sixth Edition, Chicago, IL (2004)
9. Noppakunwijai, P.; Tadros, M.K.; Ma, Z.; and Mast, R.F.; "Strength Design of Pretensioned Flexural Concrete Members at Prestress Transfer," *PCI Journal*, V. 46, No. 1, January-February 2001, pp. 34-52
10. Brewer, J. and Myers, J. J.; " Prestress Loss Behavior of High-Strength Self-Consolidating Concrete Girders Subjected to Elevated Compressive Fiber Stresses," *Proceedings for the 2008 PCI National Bridge Conference*, Orlando, FL, October 2008
11. Schindler, A.K.; Barnes, R.W.; Roberts, J.B.; and Rodriguez, S.; "Properties of Self-Consolidating Concrete for Prestressed Members," *ACI Materials Journal*, V. 104, No. 1, January-February 2007, pp. 53-61
12. PCI Interim SCC Guidelines FAST Team, *Interim Guidelines for the Use of Self-Consolidating Concrete in Precast/Prestressed Concrete Institute Member Plants*, PCI Report TR-6-03, Precast/Prestressed Concrete Institute, Chicago, IL, April 2003
13. Bentz, E.; *Response-2000 Version 1.1*, Department of Civil Engineering, University of Toronto, 2001